

UNCLASSIFIED

AD NUMBER
AD405824
NEW LIMITATION CHANGE
TO Approved for public release, distribution unlimited
FROM Distribution authorized to U.S. Gov't. agencies and their contractors; Administrative/Operational Use; MAY 1963. Other requests shall be referred to Rome Air Development Center, Attn: Electronic Warfare Lab., Research and Technology Division, Griffiss AFB, NY.
AUTHORITY
RADC ltr, 11 Oct 1966

THIS PAGE IS UNCLASSIFIED

UNCLASSIFIED

AD 405 824 _

DEFENSE DOCUMENTATION CENTER

FOR

SCIENTIFIC AND TECHNICAL INFORMATION

CAMERON STATION, ALEXANDRIA, VIRGINIA



UNCLASSIFIED

NOTICE: When government or other drawings, specifications or other data are used for any purpose other than in connection with a definitely related government procurement operation, the U. S. Government thereby incurs no responsibility, nor any obligation whatsoever; and the fact that the Government may have formulated, furnished, or in any way supplied the said drawings, specifications, or other data is not to be regarded by implication or otherwise as in any manner licensing the holder or any other person or corporation, or conveying any rights or permission to manufacture, use or sell any patented invention that may in any way be related thereto.

405824

405824

RADC-TDR-63-133



RFI REDUCTION BY CONTROL OF ANTENNA SIDELOBES

TECHNICAL DOCUMENTARY REPORT NO. RADC-TDR-63-133

May 1963

Electronic Warfare Laboratory
Rome Air Development Center
Research and Technology Division
Air Force Systems Command
Griffiss Air Force Base, New York

Project No. 4540, Task No. 454001

(Prepared under Contract No. AF30(602)-2711 by the Antenna Laboratory,
Department of Electrical Engineering, Ohio State University Research
Foundation, Columbus, Ohio)

DDC

JUN 8 1963

TISIA 2

NO OTS

When Government drawings, specifications, or other data are used for any purpose other than in connection with a definitely related Government procurement operation, the United States Government thereby incurs no responsibility nor any obligation whatsoever, and the fact that the Government may have formulated, furnished, or in any way supplied the said drawings, specifications, or other data, is not to be regarded by implication or otherwise as in any manner licensing the holder or any other person or corporation, or conveying any rights or permission to manufacture, use, or sell any patented invention that may in any way be related thereto.

The Government has the right to reproduce, use, and distribute this report for governmental purposes in accordance with the contract under which the report was produced. To protect the proprietary interests of the contractor and to avoid jeopardy of its obligations to the Government, the report may not be released for non-governmental use such as might constitute general publication without the express prior consent of The Ohio State University Research Foundation.

Qualified requesters may obtain copies of this report from the ASTIA Document Service Center, Arlington Hall Station, Arlington 12, Virginia. Department of Defense contractors must be established for ASTIA services, or have their "need-to-know" certified by the cognizant military agency of their project or contract.

FOREWORD

The research reported herein was performed in the Antenna Laboratory, Department of Electrical Engineering, The Ohio State University, under Contract No. AF30(602)-2711 between The Ohio State University Research Foundation and Rome Air Development Center, Air Force Systems Command, USAF, Griffiss AFB, N. Y. Mr. Karl Kirk of Rome Air Development Center was the contract initiator.

This report (Contractor's No. 1423-4) was written by Leon Peters, Jr., and R. C. Rudduck of The Ohio State University Antenna Laboratory.

The authors wish to express their appreciation to George H. Brown, Jr. and Phillip M. Russo who made many of the measurements and calculations.

ABSTRACT

This report describes measurements and theoretical developments on the far sidelobe or backlobe region of three basic antenna types: the horn antenna, the parabolic reflector antenna, and the Luneberg lens antenna. The application is for RFI reduction with emphasis on the use of radar absorber materials.

A technique for design of nulls in the Fresnel Zone of an aperture antenna is described and numerical examples represented. This technique has potential RFI application.

PUBLICATION REVIEW

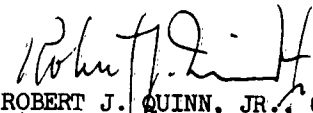
This report has been reviewed and is approved.

Approved:



for EDWARD N. MUNZER
Chief, Electronic Warfare Laboratory
Directorate of Intelligence & Electronic Warfare

Approved:



ROBERT J. QUINN, JR., Col, USAF
Director of Intelligence & Electronic Warfare

TABLE OF CONTENTS

	<u>Page</u>
I. INTRODUCTION	1
II. HORN ANTENNA	2
III. REFLECTOR TYPE ANTENNAS	4
IV. LENS ANTENNAS	10
V. FRESNEL ZONE NULLS	13
VI. CONCLUSIONS	14
BIBLIOGRAPHY	16

I. INTRODUCTION

This paper describes measurements and theoretical developments on the far sidelobe or backlobe region of three basic antenna types: the horn antenna, the parabolic reflector antenna, and the Luneberg lens antenna. The purpose is for RFI reduction with emphasis on the use of absorber materials. RFI research on the radiation patterns of antennas has been concerned with the study of sidelobes of the aperture radiation.¹ The radiation region outside line-of-sight of the aperture proper is usually large in extent and is an important region as far as RFI is concerned. Furthermore, the aperture radiation usually describes the radiation only in the vicinity of the main beam and the first few sidelobes. Outside this region, direct feed radiation and energy diffracted at the aperture edges are the dominant components.

The fact that the latter two regions are more important with regard to antenna temperature and RFI is particularly true when space communications antennas and radar antennas are considered whose main beams are often directed skywards. Then little interference is obtained due to the pattern of the aperture proper but much greater interference will be noted because of such non-aperture radiation.

The radiation in the edge diffraction region is most readily treated by the geometrical theory of diffraction. This theoretical method is employed to analyze the backlobe radiation of the horn and the parabola. Optimum parabolic antenna design is considered from the viewpoint of RFI reduction. Significant backlobe reduction by application of a limited amount of radar absorber material is experimentally demonstrated. Another method for backlobe reduction is the use of small flanges around the aperture edges. This method which demonstrates significant backlobe reduction is a wide band, low noise technique.

The source of backlobes in the Luneberg lens antenna is demonstrated and significant backlobe reduction is achieved with application of absorber material. A technique for design of nulls in Fresnel zone of an aperture antenna is described and numerical examples presented. This technique has potential RFI application.

Yet another significant undesired type of radiation occurs in the case of reflector antennas such as the parabola. This is the direct radiation from the feed which is never intercepted by the reflecting surface. This type of radiation can be reduced by one of two methods. (a) appropriate design of the feed or (b) by directly intercepting this energy by use of absorbing material placed outside the antenna proper.

This first method has been considered briefly by Caldecott et al² and it is noted that this radiation is down 45 db below the main beam for angles greater than 30°. It may also be noted that the back lobes are greater than 60 db down for angles greater than 90°. This limit is due to measuring equipment and the actual backlobe signal is not known. The second method for direct feed radiation reduction is essentially a brute force technique and is given the name of the tunnel antenna. This approach has been considered at Air Force Cambridge and Melpar³ and has not given significantly better results. The reason that full advantage of the absorber has not been obtained in these regions is probably due to edge diffraction that occurs. It should also be noted that the unwieldy tunnel antenna is certainly not applicable for the case of very large antennas that are becoming more dominant in present day technology. It should also be noted that the reduction of this tunnel concept could be significantly improved by applying some of the techniques discussed in this paper. Some new as yet untried methods for reducing this undesired direct radiation are suggested.

II. HORN ANTENNA

In the waveguide-fed rectangular horn antenna, energy is propagated substantially in the TE_{01} waveguide mode from the horn throat to the aperture. Some higher mode conversion takes place and currents are excited on the outer surface of the horn. The aperture radiation in the E-plane and in the H-plane are substantially independent of each other.⁴ With negligible mode conversion, the amplitude of the aperture distribution in the H-plane is nearly sinusoidal whereas it is nearly uniform in the E-plane. The aperture phase distribution can be determined by assuming a phase center at the horn throat with the electrical path length from the phase center to any point on the aperture determining the phase at that point, resulting in a quadratic phase distribution. Maximum directivity is obtained from a uniform phase distribution, requiring a very long horn with a small flare angle. An optimum horn design which gives a practical length without large phase error has been defined in Ref. 4. The E-plane and H-plane patterns can be calculated from the resultant aperture distribution. However, this method does not account for mode conversion and outside surface currents.

The backlobe radiation which is determined by the outside surface currents can be treated in terms of edge diffraction by means of the geometrical theory of diffraction.⁵ By this method the diffraction from each point on the aperture edge is assumed to be the same as that of the perfectly conducting half plane. Patterns calculated by the geometrical

theory of diffraction are obtained by superposition of the geometrical optics field and the edge diffracted field. The two edges perpendicular to the E-plane which will be denoted E-edges produce the diffracted field whereas the two edges perpendicular to the H-plane (H-edges) produce no diffraction because the diffraction coefficient vanishes for the H-edges. The E-plane pattern in the forward hemisphere is obtained by superposition of the geometrical optics rays with the geometrical diffracted rays from the two E-edges. The geometrical optics field in the E-plane is simply constant over the region of the included horn angle and vanishes outside this region as can be ascertained from the aperture distribution. The superposition of the geometrical diffracted rays on the geometrical optics rays produces the ripples in the main beam and the sidelobes outside the main beam. In the rear hemisphere the field is obtained from the geometrical diffracted rays alone, as it is outside the main beam in the forward hemisphere, although one edge is shielded by the horn structure over part of the backlobe region as shown in Fig. 1. Lobing caused by interference between the two edges is evident in part of the backlobe region whereas the pattern is relatively smooth in the region where shielding of one edge occurs.

The geometrical diffracted rays from the E-edges also contribute to the geometrical optics rays in planes other than the E-plane as illustrated in Fig. 2; they contribute in the conical sectors with cone angle equal to the horn angle. Thus the geometrical diffracted field contributes to the geometrical optics field in the H-plane over the main beam region and produces the backlobes over the equal-angle sector about the 180° axis. The geometrical optics field in the H-plane is sinusoidal over the included horn angle and vanishes outside. Hence this method predicts zero field outside these two sectors of the H-plane.

For experimental purposes a pyramidal X-band horn $13\frac{1}{2}$ inches in length with a $9" \times 9"$ aperture was employed. The measured antenna patterns which are shown in Fig. 3 have the general characteristics predicted by previously discussed methods.

The application of absorber to the E-edges as shown in Fig. 3a gives great reduction of the backlobes in the E-plane pattern and of the 180° lobe in the H-plane pattern as shown in Fig. 3b. Shielding of the H-edges has no significant effect on the pattern in either plane.

The diffraction at the E-edges is greatly dependent on the edge thickness; the magnitude of backlobe energy decreases rapidly with increasing edge thickness. Two $\frac{1}{2}$ inch flanges were added to the E-edges of the experimental horn so as to increase the edge thickness

from 5/64 inch to 1/2 inch. The reduction of edge diffraction is evident in Fig. 3a and amounts to 10 db over 180 degrees of aspect. It should be noted that this type of reduction should be relatively insensitive with respect to frequency and the concept could be enhanced by the introduction of additional edges. Further reduction could also be obtained by application of absorber.

It is recommended that further studies of the horn and diffraction by such edges be conducted to determine optimum edge configurations. These studies should yield results applicable not only to the horn but to other antennas as is demonstrated in the following, by application to the parabola.

III. REFLECTOR TYPE ANTENNAS

The radiation from a reflector antenna can be characterized by three regions as illustrated in Fig. 4. The desired radiation which we shall define as the aperture radiation consists of the main beam and its side lobes. Control of these side lobes is accomplished by means of controlling the aperture distribution. It may be noted that this control is limited for very large antennas by construction tolerances. If the antenna construction is not sufficiently accurate, phase errors are introduced which lead to greatly increased side lobes. The tolerance requirements have been discussed by Jacobs.¹ A survey of some characteristics of reflector antennas has been given by Truske.⁶

We define the second type of radiation as direct radiation and is due to the energy radiated by the feed antenna which is not intercepted by the reflecting surface. This is an undesired type of radiation. Direct radiation can be reduced by feed antenna design or by direct interception of this energy in some manner which usually results in large unwieldy structures. The third type is also undesired and we define it as edge diffracted radiation. In this case the feed illuminates an edge of the reflector which then diffracts this energy throughout space in a manner similar to the horn discussed previously. These three regions are illustrated in Fig. 4 for the paraboloidal reflector antenna which has been chosen as a special case of this more general class of antennas.

The desired aperture radiation is basically controlled by the reflector size, the ratio of focal length to reflector diameter (F/D), and the feed pattern. These parameters determine the aperture distribution which, in turn, controls the tradeoff between gain and sidelobe level. The sidelobe level and the gain both decrease with increasing center to edge aperture taper. Aperture radiation has been extensively studied.

The direct feed radiation is the dominant component in the spill-over region where the reflector does not intercept the feed radiation and the sidelobes of the aperture radiation are low relative to the feed radiation. In a reflector of large F/D , the direct feed radiation can be maintained at a low magnitude with a narrow feed pattern, resulting in a high center to edge aperture taper. If a small center to edge taper is desired, then maintaining low direct feed radiation requires a large feed in order to obtain a steep slope in the feed pattern in the direction of the reflector rim. The large feed requirement results in high aperture blocking by the feed which is usually accompanied by increase in sidelobes, particularly in small reflector sizes. However, in reflectors of small F/D , a small center to edge taper can be maintained with low direct feed radiation even with small feeds. Actually, there is an optimum F/D for a given reflector diameter which allows minimum feed size. The relationships between the incident and reflected energy at the rim are shown in Fig. 5. For a given slope in the feed pattern at the rim, minimum direct feed radiation occurs for a maximum value of $d(2\alpha)/ds$ where ds is an incremental arc length along the reflector. Since α is given by

$$(1) \quad \tan \alpha = - \frac{x}{2F} \quad \bigg|_{x = \frac{D}{2}} = - \frac{D}{4F}$$

then

$$(2) \quad \frac{d(2\alpha)}{ds} \quad \bigg|_{x = \frac{D}{2}} = 2 \frac{d\alpha}{dx} \frac{dx}{ds} \quad \bigg|_{x = \frac{D}{2}} = - \frac{4}{D} \sin \alpha \cos^2 \alpha.$$

The quantity $(-\sin \alpha \cos^2 \alpha)$ is plotted in Fig. 6 where the maximum value occurs at $\alpha = -35 \frac{10}{4}$. Thus the optimum value of F/D which gives minimum direct feed radiation for a fixed feed pattern slope in the rim direction is obtained from Eq. (1) as 0.353.

The third radiation region which is denoted edge diffraction corresponds to the energy which is diffracted around the reflector rim. The magnitude of edge diffraction is proportional to the feed radiation incident at the reflector rim. Thus, if in reduction of direct radiation the incident energy in the rim direction is reduced, edge diffraction is also reduced. Usually the reflector diameter and the center to edge taper are first specified. Hence, the relationship between the incident energy at the edge and at the center are shown in Fig. 7 for a fixed aperture taper and fixed reflector diameter. For a center to edge aperture taper T and a feed voltage pattern $A(\theta)$ the incident field intensity at the reflector is given by $A(0)/F$ in the on-axis direction and by $A(0)/FT$ in the rim direction. By the geometrical theory of diffraction, the diffracted ray (measured in field intensity) in the back-lobe direction (180°) is given by

$$(3) \quad U_d = \frac{K_1 A(0)}{FT} \sqrt{-\frac{D}{2k} \csc 2\alpha (\csc \alpha \pm 1)}$$

$$= \frac{K_2}{T} \sqrt{-\csc 2\alpha (\csc \alpha \pm 1)}$$

where the + sign applies to polarization parallel to the edge, - sign to perpendicular polarization and

K_1, K_2 = proportionality constants

$$k = \frac{2\pi}{\lambda}$$

The quantities $\sqrt{-\csc 2\alpha (\csc \alpha \pm 1)}$ are plotted in Fig. 8 in which a minimum occurs at $\alpha = -55\frac{1}{2}^\circ$ for perpendicular polarization and $\alpha = -90^\circ$ for parallel polarization. Thus the optimum F/D for minimum backlobe radiation (perpendicular polarization) is given by 0.172 under the assumptions of constant reflector diameter and constant center to edge taper.

Actually this optimum F/D does not take into account the slope of the feed pattern at the rim. As previously described, the optimum F/D for minimum direct feed radiation occurs for a maximum value of $d(2\alpha)/ds$. Since the backlobe radiation is proportional to the rim-directed feed radiation, the viewpoint can be taken that minimum backlobe radiation occurs for minimum direct feed radiation. Since the optimum F/D under these two criteria are not the same, the true optimum for minimum edge diffraction is intermediate to these two values.

The fact that the optimum F/D for minimum backlobe radiation lies between 0.172 and 0.353 demonstrates the reason that very low noise temperatures have been measured in parabolic reflector antennas with small F/D .⁷

The behavior of the three radiation regions as a function of reflector size can be evaluated by maintaining constant F/D and hence constant α , and identical feed pattern. This situation is illustrated in Fig. 9 in which it is evident that the relative aperture illumination (field intensity) remains the same although it is proportional to $1/D$ for equal total energy. Under these assumptions, the on-axis power density or antenna gain above isotropic is proportional to the aperture area. Each sidelobe maximum is also proportional to the aperture area and thus the ratio of a sidelobe maximum to the pattern maximum is equal to the ratio of the corresponding sidelobe maximum of the other pattern to its pattern maximum. However, the corresponding sidelobes are not coincident in direction and the absolute level of the sidelobe maxima are nearly equal in any given direction. This means that although the relative magnitude of the corresponding sidelobes remain the same as the aperture size is increased, the sidelobes move closer to the main beam, resulting in approximately equal absolute sidelobe power in a given direction as shown in Fig. 10. This effect can easily be shown for a uniformly illuminated square aperture in which the absolute field intensity for a constant input power is given by

$$(4) \quad E(\theta, 0) = \frac{2 \sin(\frac{1}{2}ka \sin \theta)}{k \sin \theta} .$$

The pattern maximum is given by

$$(5) \quad E(0, 0) = a$$

and the sidelobe maxima are given by

$$(6) \quad E(\theta_m, 0) = \frac{2}{k \sin \theta} = \frac{\lambda}{\pi \sin \theta} .$$

The direct feed radiation remains the same because identical feed patterns and F/D are used. The edge-diffracted radiation is shown in Fig. 9 in which the backlobe level is given by

$$(7) \quad U_d = \frac{KA(2\alpha)}{\frac{kD}{2} \csc 2\alpha} (\csc \alpha + 1).$$

Thus the edge diffraction power density is proportional to $1/D$. The expression of Eq. (7) assumes that the edge thickness is very thin compared to a wavelength but the comparison is valid for a constant edge thickness. However as the reflector diameter increases, the edge thickness tends to increase.

In summary, the behavior of the three radiation regions is as follows: Relative to the pattern maximum the power level in the edge diffraction region is proportional to $1/D^3$ whereas the power levels in the sidelobe and direct feed radiation regions is proportional to $1/D^2$.

Since the effect of reflector size on the radiation regions of a parabolic reflector antenna has been described above, a small reflector antenna can be employed for experimental purposes and the results extrapolated. A 14 inch diameter reflector with a focal length of 3 inches was chosen for use at X band.

Two of the feeds employed were the waveguide double-dipole feed as described by Silver⁸ and an open-ended X band waveguide feed with a 3 inch diameter circular flange; the corresponding feed patterns are shown in Fig. 11. The lower backlobe and direct feed radiation with use of the flange feed is evident from the antenna patterns of Fig. 12. It is also noted that the flange feed pattern is symmetrical in the E and H planes.

The use of absorber material to reduce edge diffraction was measured for several absorber configurations. By examination of the edge diffraction coefficients for the two polarizations, perpendicular and parallel to the edge, it is apparent that little edge diffraction occurs in the H plane, which is confirmed by measurements. With the 14 inch reflector and flange feed, significant reduction of backlobe radiation in the E plane (10 db over 100 degrees) is shown in Fig. 13 for absorber placed around the entire reflector rim. The fact that the portion of the rim perpendicular to the E plane produces most of the edge diffraction is also illustrated in Fig. 13. For a limited amount of absorber placed over this portion of the rim, the backlobe reduction is nearly as great as with the full use of absorber.

It should be noted that direct feed radiation can be significantly reduced by placing a reflecting array at the direction in which reduction

is desired. The closer the array is placed to the feed antenna the more reduction is obtained. One such experiment yielded a reduction of 8 db over 60 degrees. Similar reduction has been obtained by placing a shield over the feed but these methods are extremely makeshift and usually introduce aperture blocking and thus increased side lobes for the aperture radiation. A better approach should be concerned with the feed design itself. In particular, methods of obtaining the desired feed pattern without introducing aperture blocking are needed. This certainly sounds contradictory since a more controlled pattern requires a larger feed antenna.

However, a proposed technique for such feed design is illustrated in Fig. 14. This technique consists of the use of a surface wave structure which is placed in the antenna aperture so as to align with the feed. Any direct feed radiation should be entrapped by the surface wave structure and propagated outside the reflector rim where it can be absorbed or re-directed. Since the direct feed radiation which illuminates the edge should also be entrapped, reduction of backlobes should be achieved. In one approach a dielectric sheet structure of $\lambda/4$ design would be used so that the energy reflected from the reflector could be transmitted with negligible attenuation and reflection. Any effect of reflections from the sheet would simply be eliminated by antenna tuning. A second approach would be a sheet of thin space cloth so that negligible effect would be produced on the reflected energy because of its normal incidence. The direct feed radiation has a highly oblique incidence and the resultant greater path length in the absorber should produce high attenuation of this component.

In conclusion, great reduction of backlobes has been demonstrated with the use of a limited amount of absorber material. A flange technique has also demonstrated great backlobe reduction.

It is recommended that the edge diffraction study of the parabolic antenna continue and that possible optimum edge configurations be developed for use in low noise applications as well as in RFI reduction.

IV. LENS ANTENNAS

Many antennas depend on lens action to obtain the aperture distribution and as we have defined it - the desired aperture radiation. This would appear to be a rather simple problem to reduce the various types of undesired radiation for RFI purposes since the feed is outside the region in which the desired radiation propagates, no aperture blocking appears. Thus it would appear that relatively simple methods would make it possible to eliminate all of the undesired radiation. However the lens structure usually contains discontinuities which drastically upsets this simple picture. An example is the Luneberg lens.

In the most common Luneberg lens the energy from a feed on the lens rim is focussed into a collimated beam by refraction of energy within the lens as shown in Fig. 15. The lens action is accomplished with a dielectric variation given by

$$(8) \quad \epsilon(r) = 2 - r^2, \quad 0 \leq r \leq 1$$

which is a function only of radius. Since the lens is circularly symmetric, the beam can be scanned by feed movement alone or multiple beams can be obtained by use of multiple feeds. In the ideal lens the backlobe radiation would be entirely caused by the feed. Thus the backlobe radiation could be decreased by reduction of the feed backlobes, e.g., by use of techniques described in Section II on the horn antenna. Thus, ideally, the backlobes of a large Luneberg lens antenna could be easily reduced. However, in the practical construction of a Luneberg lens the dielectric variation is usually achieved by use of many concentric uniform shells; each shell has a dielectric constant corresponding to its mean radius. A contribution to the backlobe radiation is made by scattering from the shell interfaces. The antenna patterns for an 18-inch diameter commercial lens at $f = 10$ gc are shown in Fig. 16. This lens has 24 shells with a typical shell thickness of 1/2 inch with some thicknesses as low as 1/10 inch. The feed employed was an open ended X band waveguide flared in the E-plane to give a $3/4" \times 1"$ aperture. For this configuration, the backlobe contributions from the feed and the shell interfaces are about equal. Reduction of the feed backlobes by shielding the feed with absorber gives a slight backlobe reduction as shown in Fig. 16. Shielding the entire rear hemisphere of the lens gives the reduction also shown in Fig. 16.

An understanding of the backlobe contribution from the shell interfaces can be obtained by calculation of the contribution from each shell.

The scattering from the interface, farthest from the feed, of a given shell will be assumed to be the same as that of a homogeneous dielectric sphere having the same dielectric constant as the shell and which is embedded in a dielectric medium with dielectric constant equal to that of the outer adjacent shell. This component of the scattered power from the i th shell (where the shells are numbered with increasing radius) is then approximated by

$$(9) \quad p_{sc} = k_i \pi a_i^2$$

where

a_i = shell outer radius

$$k_i = \frac{\sqrt{\epsilon_i} - \sqrt{\epsilon_i + 1}}{\sqrt{\epsilon_i} + \sqrt{\epsilon_i + 1}}$$

and ϵ_i is obtained from Eq. (8) with

$$(10) \quad r = \frac{1}{2} (a_i + a_{i-1}) .$$

The assumption that the incident energy is a plane wave within the lens is not good for the interfaces nearest the feed because the back surfaces of the lens is not the far field of the feed antenna. The power from an interface nearest the feed can be expressed as

$$(11) \quad p_{sc} = C_i \pi k_i a_i^2$$

where the value of C_i would not vary greatly from unity. Summation of the contribution from each shell under the assumption that the contributions add incoherently gives the total power scattered from the shell interfaces as

$$(12) \quad P_{sc} = \sum_{i=1}^N k_i \pi a_i^2 (1 + C_i) .$$

The absolute gain level of the scattered power is given by

$$(13) \quad G_{sc} = \frac{P_{sc}}{P_i}$$

where P_i is incident power intercepted by the lens. For an incident plane wave of unit power density the incident power is equal to the effective lens aperture or

$$(14) \quad P_i = A = \pi a^2$$

The gain of the beam maximum is

$$(15) \quad G = \frac{4\pi}{\lambda^2} A$$

Thus the relative backlobe radiation is given by

$$(16) \quad \frac{G_{sc}}{G} = \frac{\lambda^2}{4A^2} \sum_{i=1}^N k_i a_i^2 (1 + C_i)$$

The magnitude of Eq. (16) was calculated for the lens of Fig. 16 by using the measured shell radii. For $C_i = 0$, the calculation gave $G_{sc}/G = -43\frac{1}{2}$ db. Since a reasonable mean value for C_i would be approximately unity, then G_{sc}/G would be about 3 db above the $-43\frac{1}{2}$ db level, giving a value of G_{sc}/G of about -40 db.

Lens antennas in general and the Luneberg lens in particular then do not lend themselves to reduced undersired radiation or to RFI reduction of this nature. This is because of the discontinuities in the lens structure.

V. FRESNEL ZONE NULLS

In the Fresnel region of an antenna the usual characteristic side-lobes have not yet been formed. However, deep minima can appear in this region due to aperture blocking. For example, they could be introduced in the Fresnel zone pattern of a parabolic antenna by feed blocking or by application of absorber material. This type of minima might be used for RFI reduction. In particular, if a large stationary antenna is to be used as a relay it might be desirable to operate some other installation in its vicinity. Thus, if a null could be created in the radiation of that antenna at the position of the other installation than a significant interference reduction is obtained.

The necessary aperture blocking can be accomplished by application of radar absorber material (RAM) to some small area in the antenna aperture. In this case the total fields are given by

$$(17) \quad E^t = E^{RAM} + E^{ANT}$$

where E^{ANT} is the unperturbed antenna field and E^{RAM} is the field due to the absorber. Since the total field is zero at the absorber then E^{RAM} is the negative of the field radiated by the blocked portion of the aperture. Thus, in order to obtain a null at a specific location the blocked portion must be chosen so that its field contribution is equal to E^{ANT} , both fields at the desired null location.

The approximate position and size of the blocked portion of the aperture can be obtained as illustrated in Fig. 17. Blocking is to occur on an aperture plane of constant phase. The approximate position of the portion to be blocked is obtained by requiring the electrical path length from the desired null location to this aperture plane to give a phase delay equal to the phase difference between E^{ANT} and the aperture plane phase. The approximate area of the blocked portion is obtained by assuming a uniform aperture field in this vicinity and calculating the area required to produce a radiated field at the desired null location equal in magnitude to $|E^{ANT}|$.

In order to determine the blocked portion more precisely, the aperture is subdivided into square meshes with the assumed field constant in each mesh. Then the magnitude and phase of the field at the desired null location is calculated as contributed by each mesh. Small changes in the size and position of the blocked area can then be made to produce the desired null.

As a numerical example of this technique a circular antenna aperture of diameter 16.5λ and having a $(1-r^2)$ aperture distribution was selected. The desired null position is chosen 50λ from the aperture plane and 12.7λ from the symmetry axis. The Fresnel pattern is given in Fig. 17. An estimate of the blocked aperture portion is obtained from the approximate method. The actual null produced by the estimated block was calculated by use of a computer program. The minimum is found to be 0.78λ from the desired null location and it is not deep as illustrated in Fig. 18. Precise adjustment of the blocked portion gives improved depth and location of the minimum as indicated in Fig. 19.

It should be noted that although this technique will not appreciably affect the main beam the sidelobes may significantly increase.

VI. CONCLUSIONS

The radiation patterns of the horn antenna are explained by the use of the geometrical theory of diffraction. Only two of the four edges produce significant edge diffraction. Significant reduction (10 db over 180 degrees) of backlobe radiation is achieved by application of a limited amount of absorber. Significant reduction is also achieved by the use of small flanges on the aperture edges. The flange technique is wide-band and is good for low noise applications, e.g., the ground-based Hogg horn antenna used for satellite communications.

An optimum focal length to diameter ratio (F/D) is derived for the parabolic antenna on the basis of minimum direct feed radiation. The effect of feed pattern on edge diffraction is described. An optimum value of F/D is derived for minimum edge diffraction. The two optimum values of F/D indicate a small F/D is best with respect to RFI considerations. The effect of reflector diameter on the radiation in the three radiation regions is shown, allowing research results to be generalized in terms of antenna size. Measured results on an experimental model demonstrate the reduction of the direct feed radiation and the edge diffraction with improvement in the feed pattern. This feed pattern is symmetrical in the E and H planes. Use of the geometrical theory of diffraction indicates the portions of the reflector rim which produce most of the edge diffraction. Measurements with the use of a limited amount of absorber material confirm the theoretical results. The limited absorber gives nearly as much reduction (10 db over 120 degrees) as does the use of absorber over the entire reflector rim.

The source of backlobe radiation of the Luneberg lens antenna is demonstrated to be the structural discontinuities of the shell type construction. The feed backlobes may also contribute but they can be easily reduced. A method for calculation of the scattering from the shell interfaces is presented and the calculations are in good agreement with measurements. Significant reduction in backlobes was obtained with use of absorber over the entire rear hemisphere of the lens.

A technique for design of nulls in the Fresnel zone of an aperture antenna is described. Numerical examples of this technique are given.

BIBLIOGRAPHY

1. Jacobs, E., "Predicting The Antenna's Role In RFI," Electronic Industries, Vol. 19 No. 5, May 1960, p. 98.
2. Caldecott, R. and Brown, D. M., "The Design of Low Noise Antennas for Tropospheric Scatter Reception," 15 January 1960 (AD-236- 181) Report 904-1, Antenna Laboratory, The Ohio State University Research Foundation; prepared under Contract DA 18-119-sc-533, U.S. Army Signal Procurement Office, 9800 Savage Road, Fort George G. Meade, Maryland.
3. "Final Report On Theoretical And Experimental Investigations On Methods Of Reducing Antenna Side Lobes," Melpar Inc., AF 19(604)-1898, AD 152394VC, June 15, 1958.
4. Kraus, J. D., Antennas, McGraw-Hill Book Co., 1950 p. 371-381.
5. Keller, J. B., "Diffraction By An Aperture," Jour. Appl. Phys. Vol. 28, No. 4, pp. 426-444, April 1957.
6. Truske, T., "Reducing The Effects Of Sidelobe Signals," John Hopkins Univ., Baltimore, Md., Master's Thesis, 1961.
7. Pauling-Toth, I.I.K., et al, "The Use Of A Paraboloidal Reflector Of Small Focal Ratio As A Low-Noise Antenna System," Proc. IRE(Correspondence) Vol. 50, No. 12, December 1962, p. 2483.
8. Silver, S., Microwave Antenna Theory And Design, McGraw-Hill Book Co., Inc., New York, p. 255, 1949.

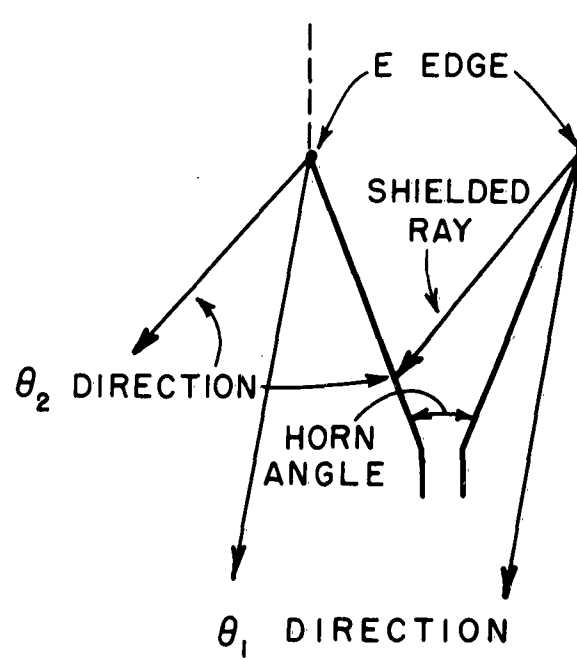


Fig. 1. Edge diffraction in E plane of horn antenna.

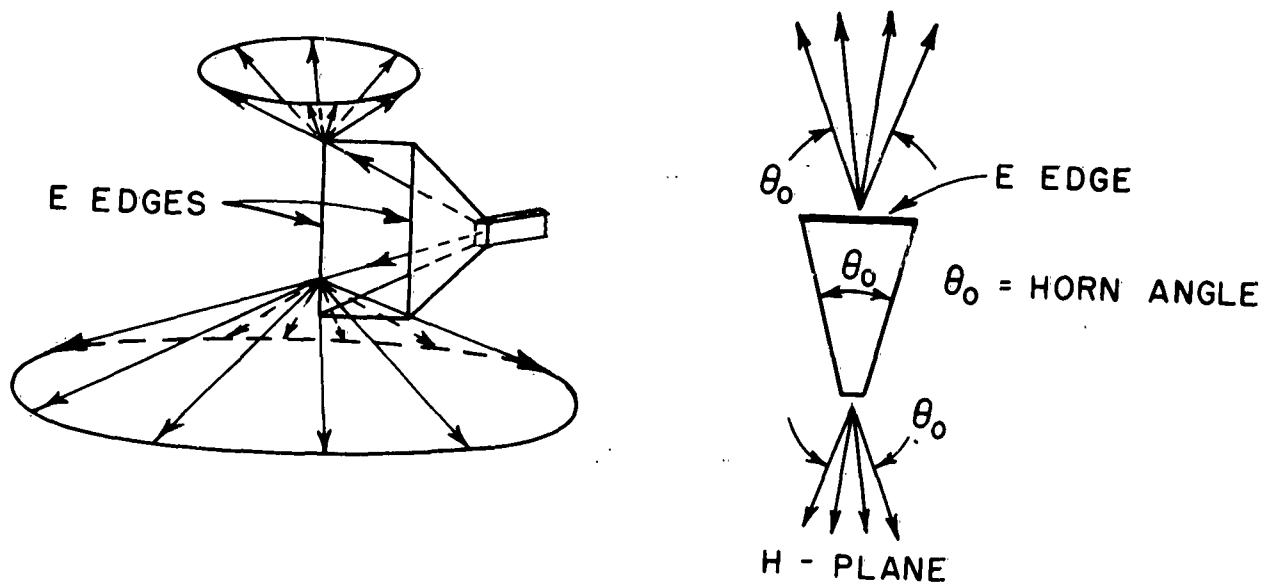


Fig. 2. Edge diffraction from pyramidal horn antenna.

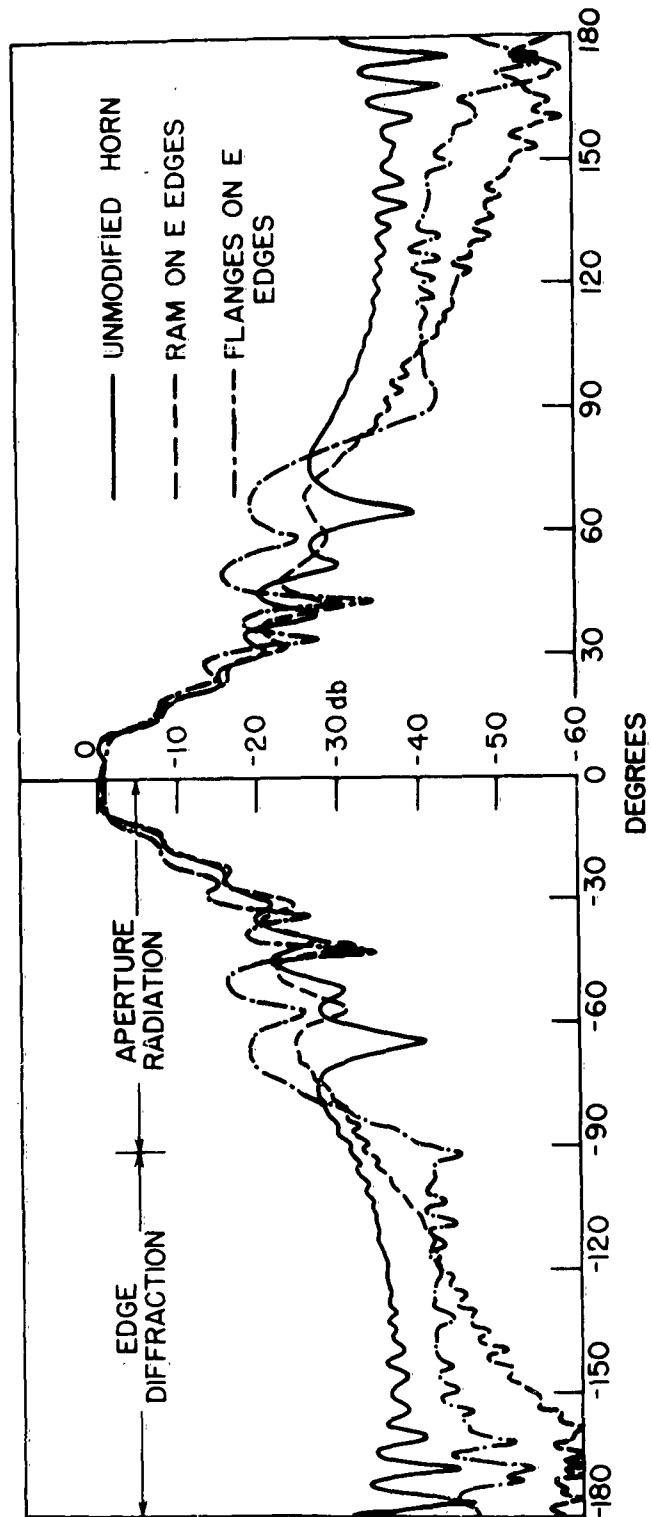


Fig. 3. Pyramidal horn antenna patterns
(a) E-plane.

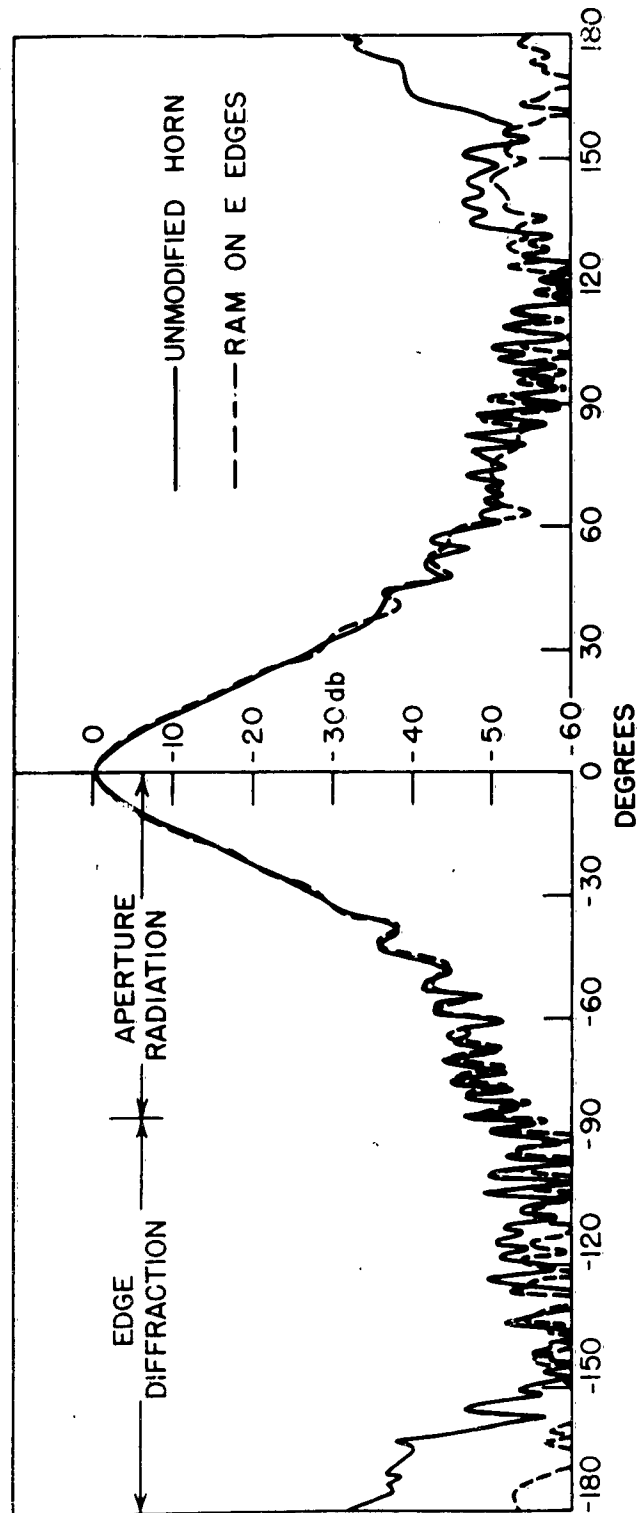


Fig. 3. Pyramidal horn antenna patterns
(b) H-plane.

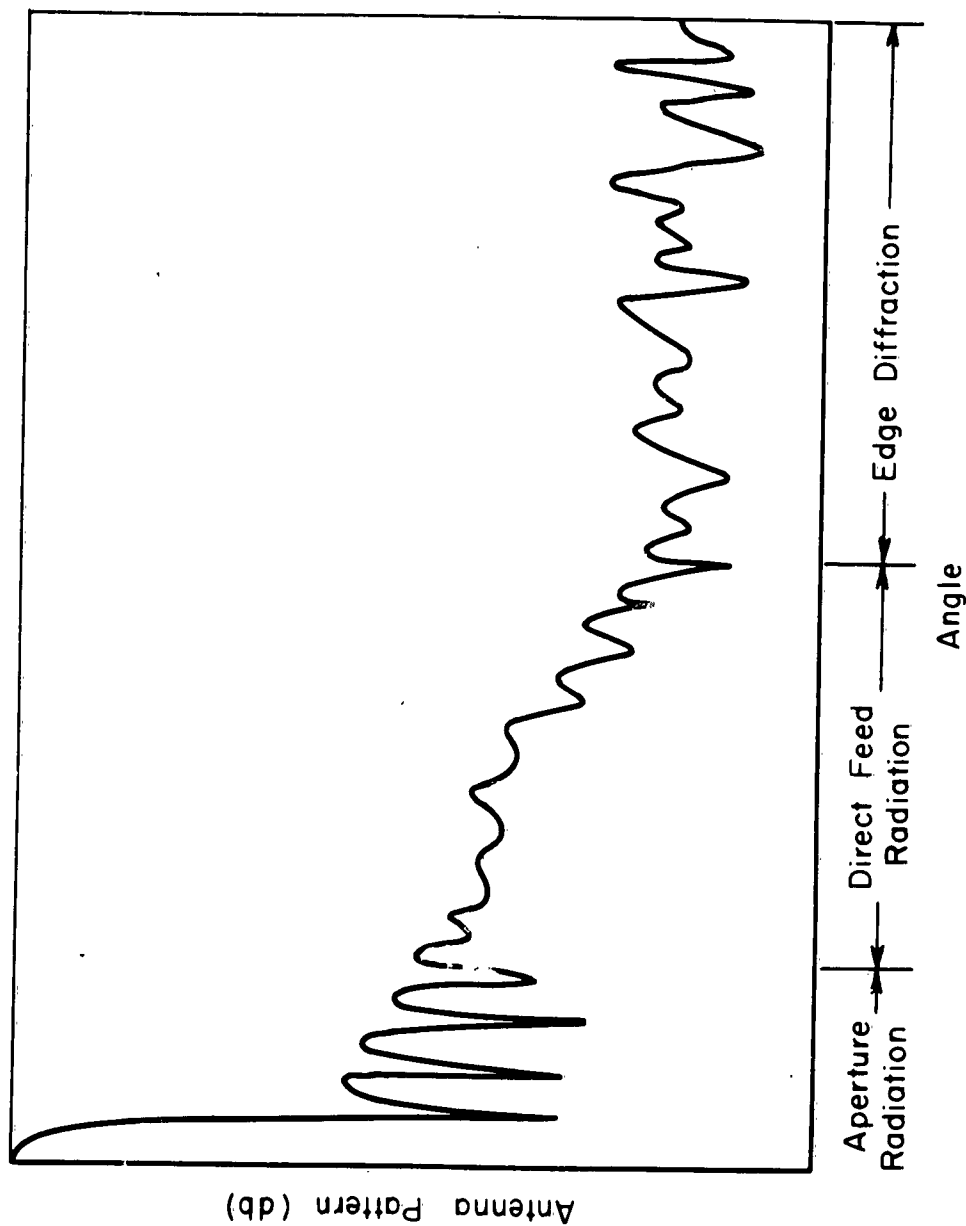


Fig. 4. Radiation regions of parabolic reflector antenna.

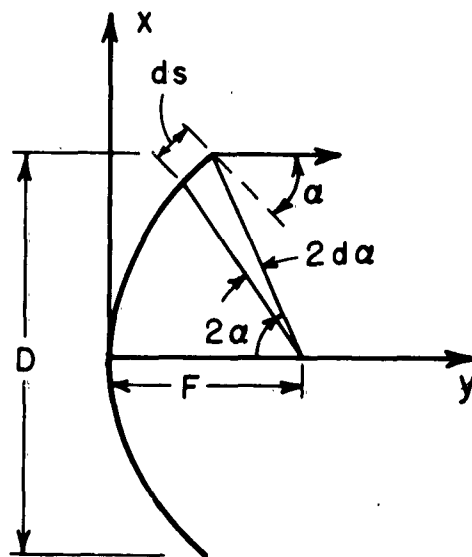


Fig. 5. Angular relationships in a parabolic reflector.

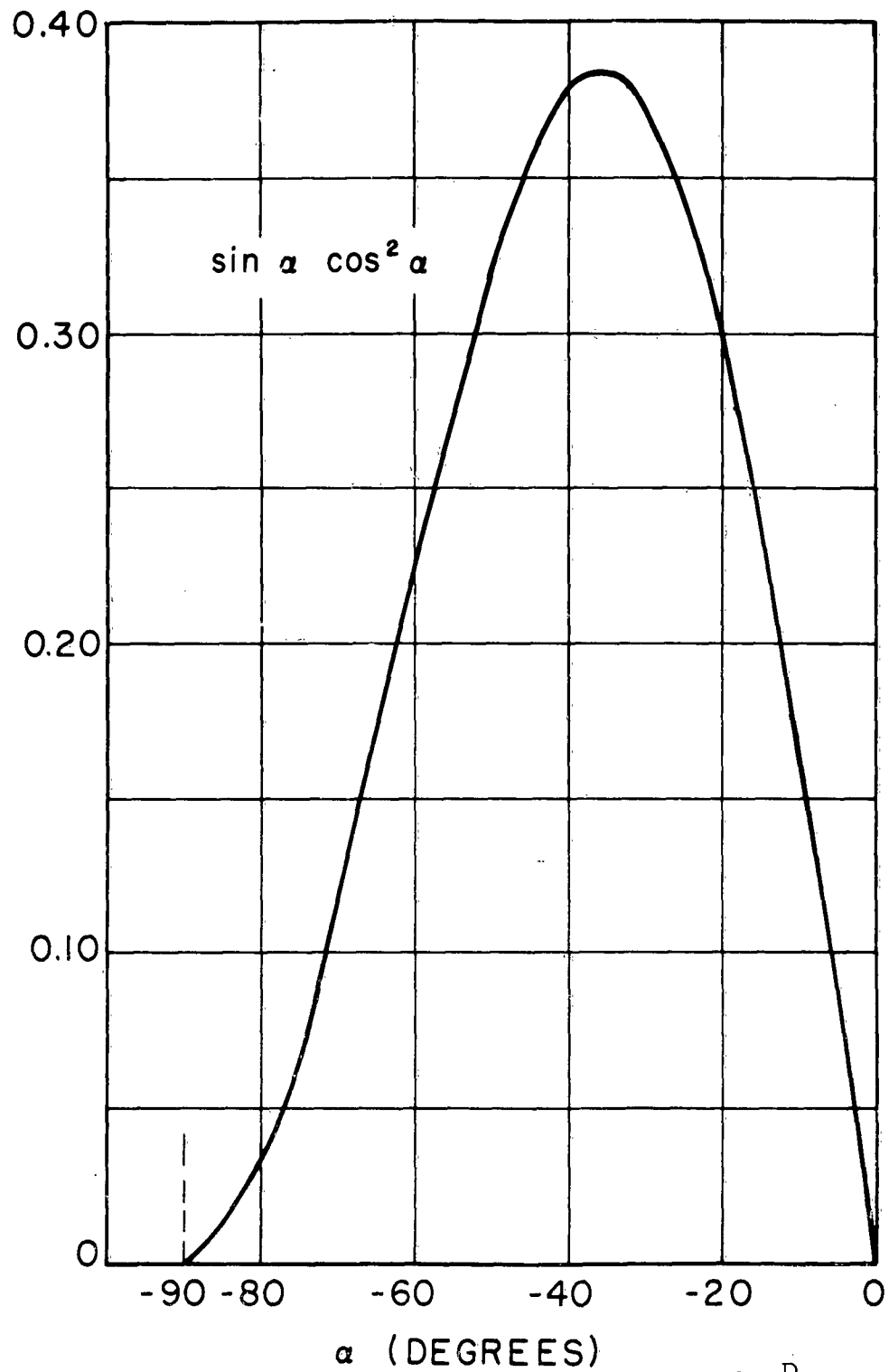


Fig. 6. Variation of direct feed radiation with $\alpha = \tan^{-1} \frac{D}{4F}$
 $(-\sin \alpha \cos^2 \alpha)$.

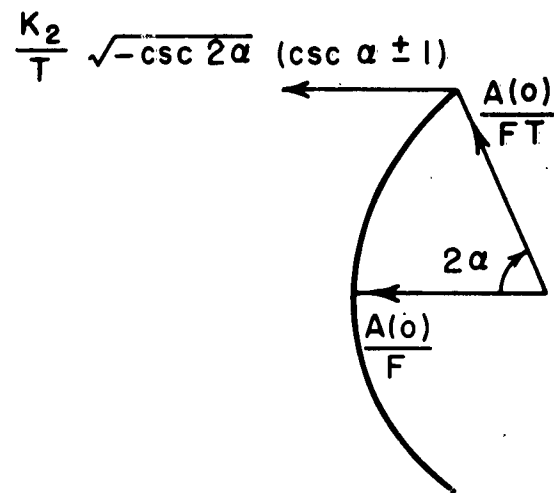


Fig. 7. Field relationship at reflector rim for fixed D .

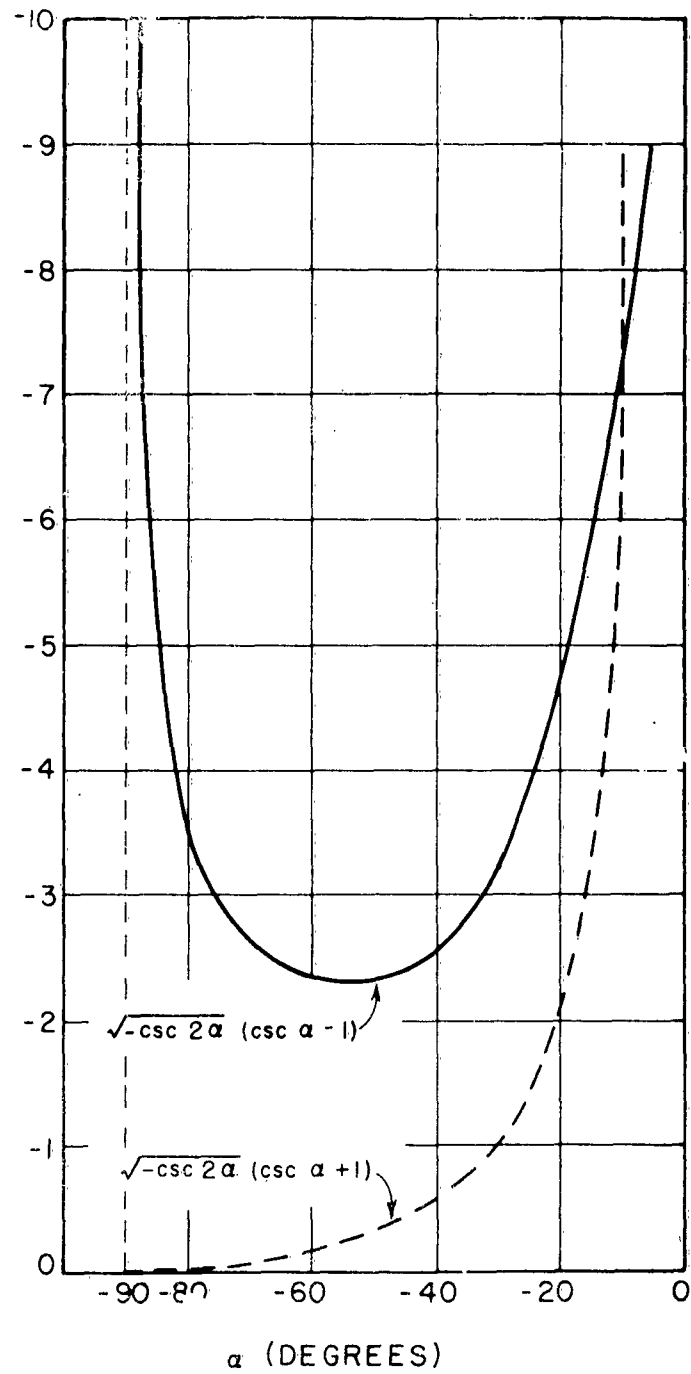


Fig. 8. Backlobe radiation as a function of $\alpha = -\tan^{-1} \frac{D}{4F}$
 $(\sqrt{-\csc 2\alpha} (\csc \alpha \pm 1))$.

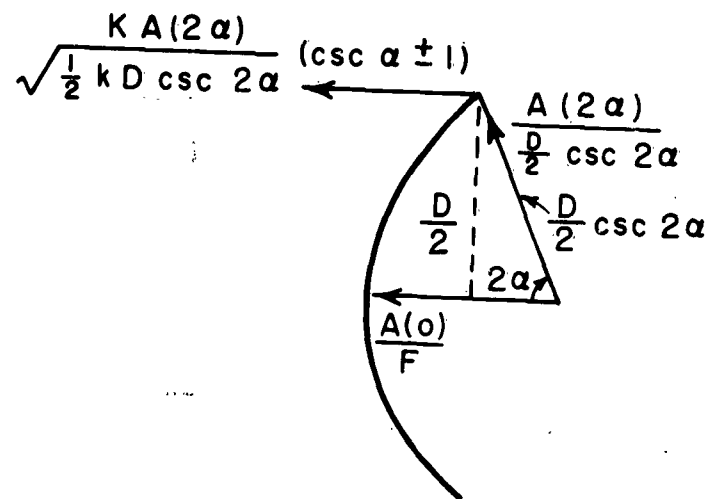


Fig. 9. Field relationships at reflector rim for fixed F/D .

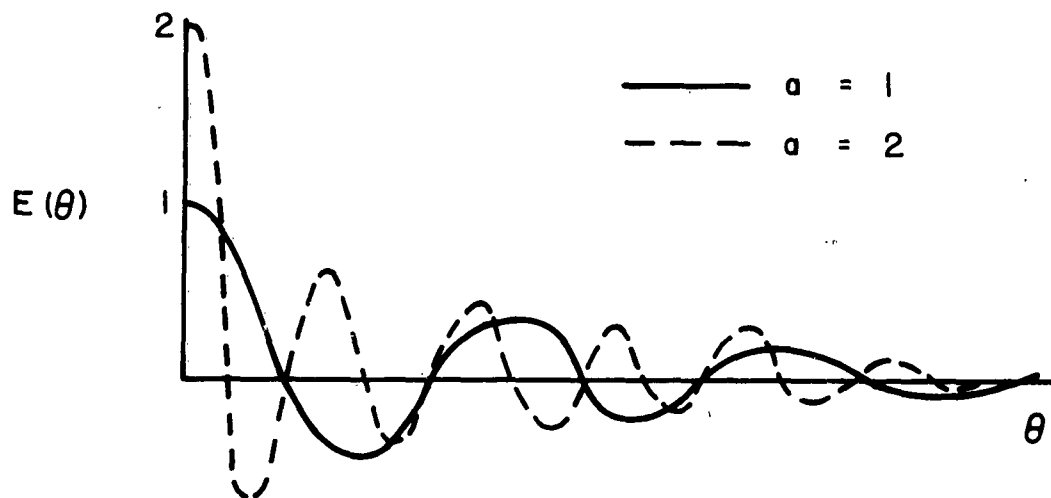


Fig. 10. Effect of antenna size on aperture radiation.

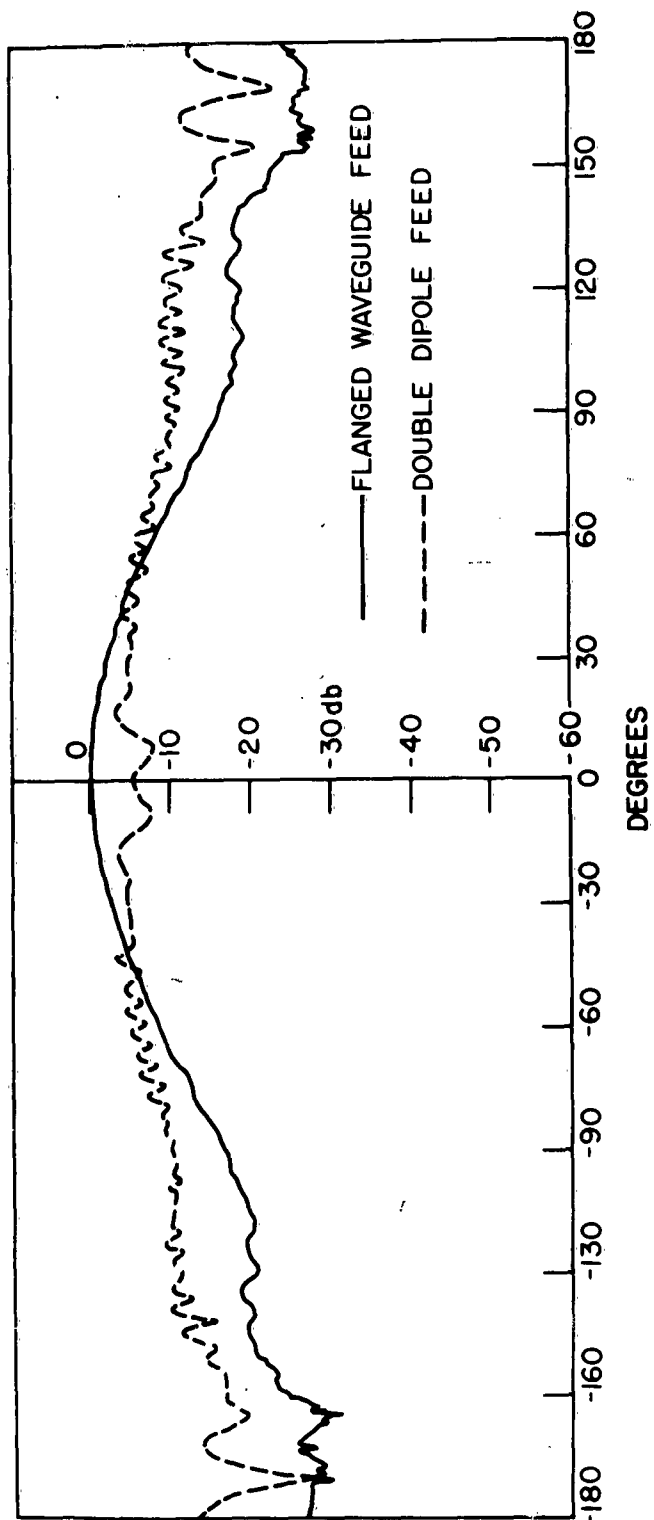


Fig. 11(a). Feed patterns.

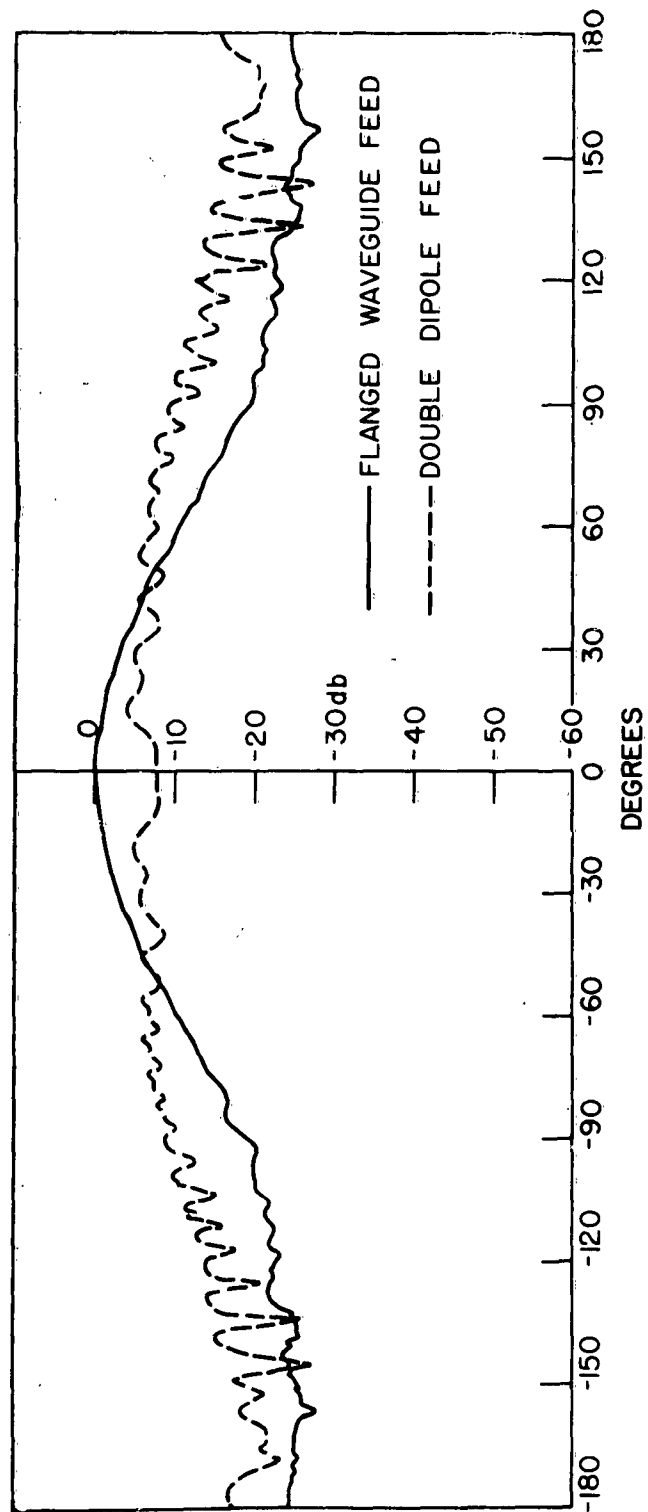


Fig. 11(b). Feed patterns.

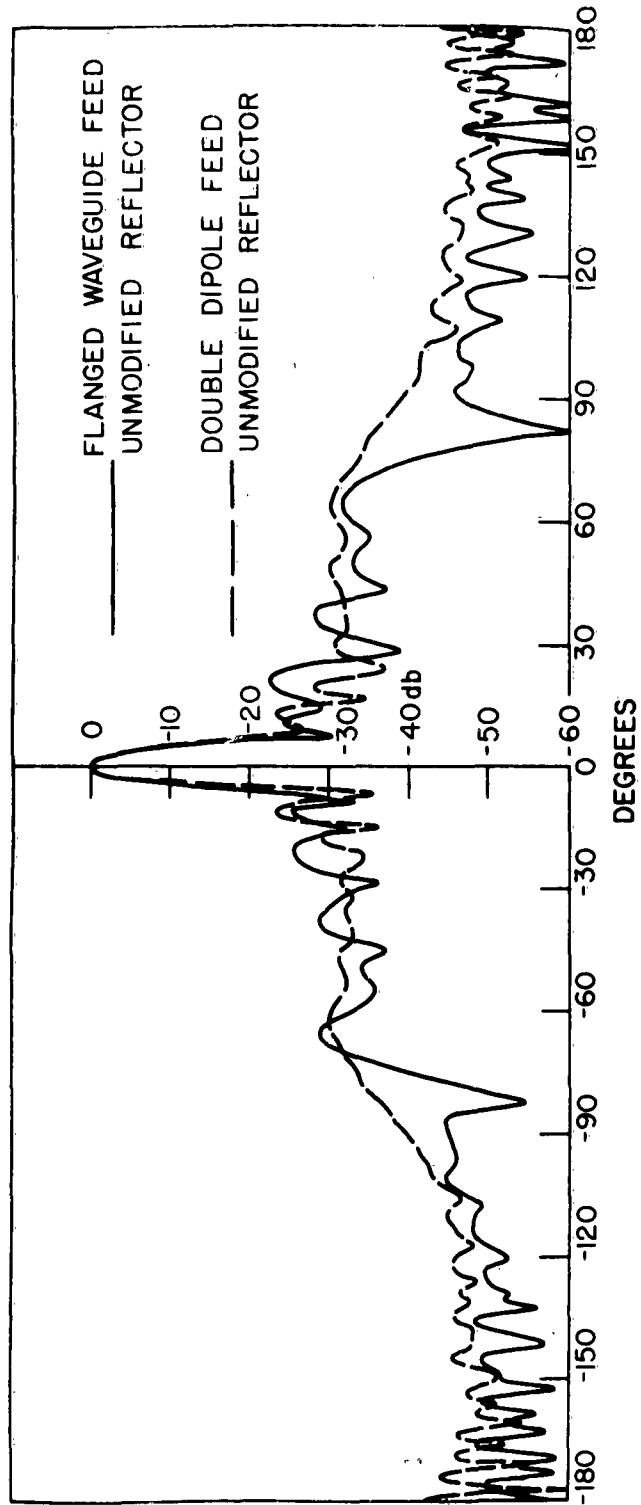


Fig. 12. Parabolic antenna patterns.

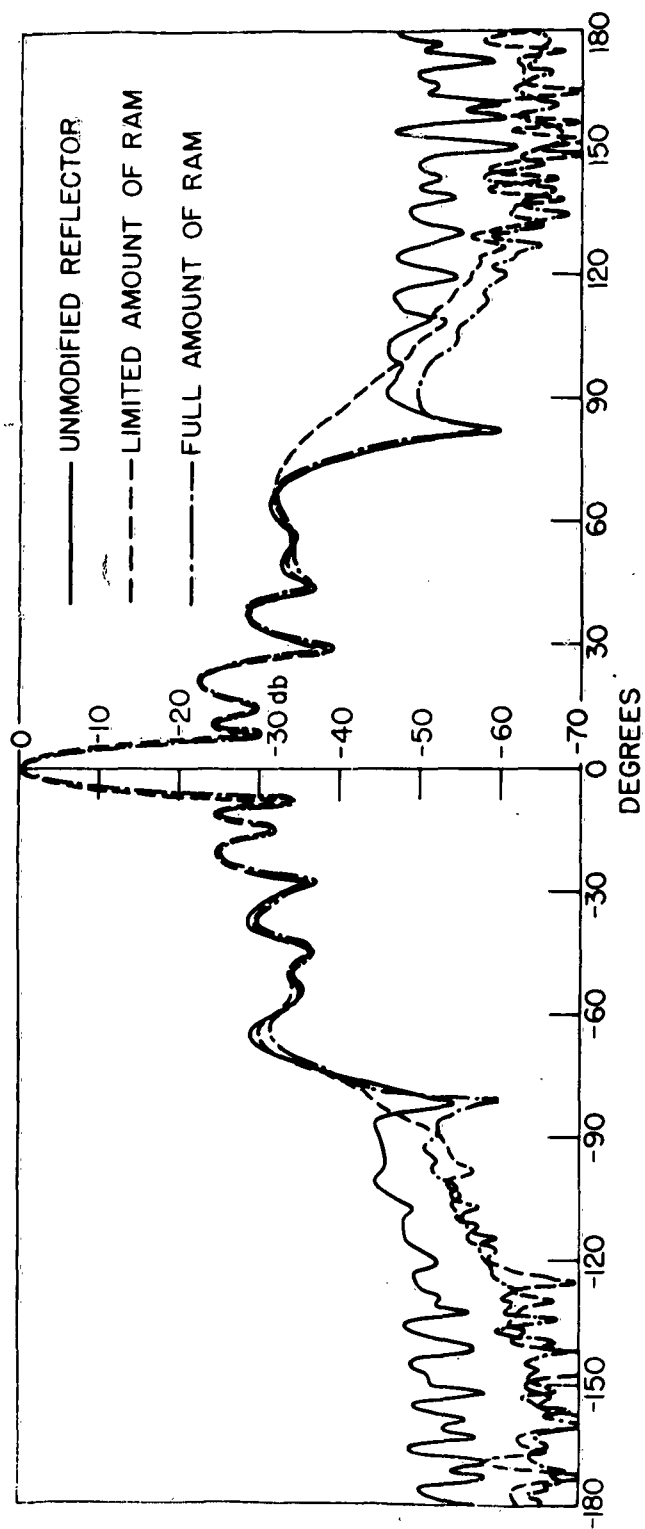


Fig. 13. Parabolic antenna patterns.

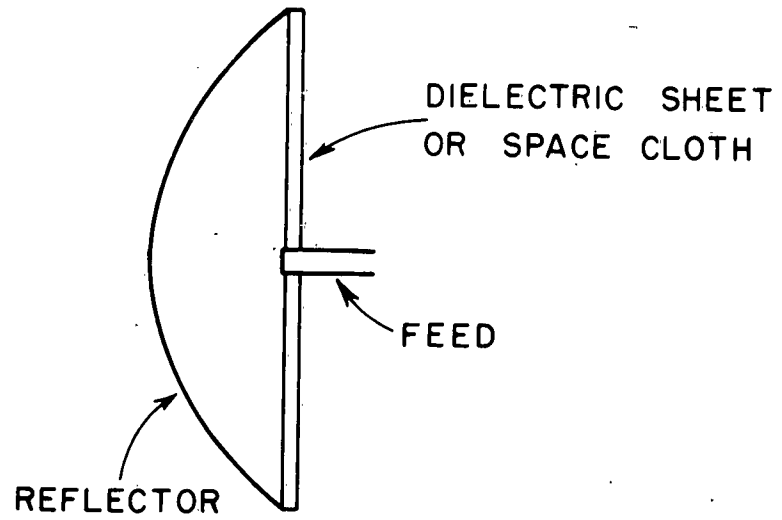


Fig. 14. Proposed technique for reduction of direct feed radiation and edge diffraction.

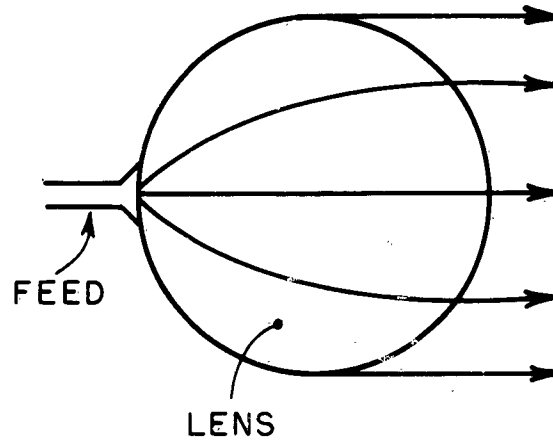


Fig. 15. Luneberg lens antenna.

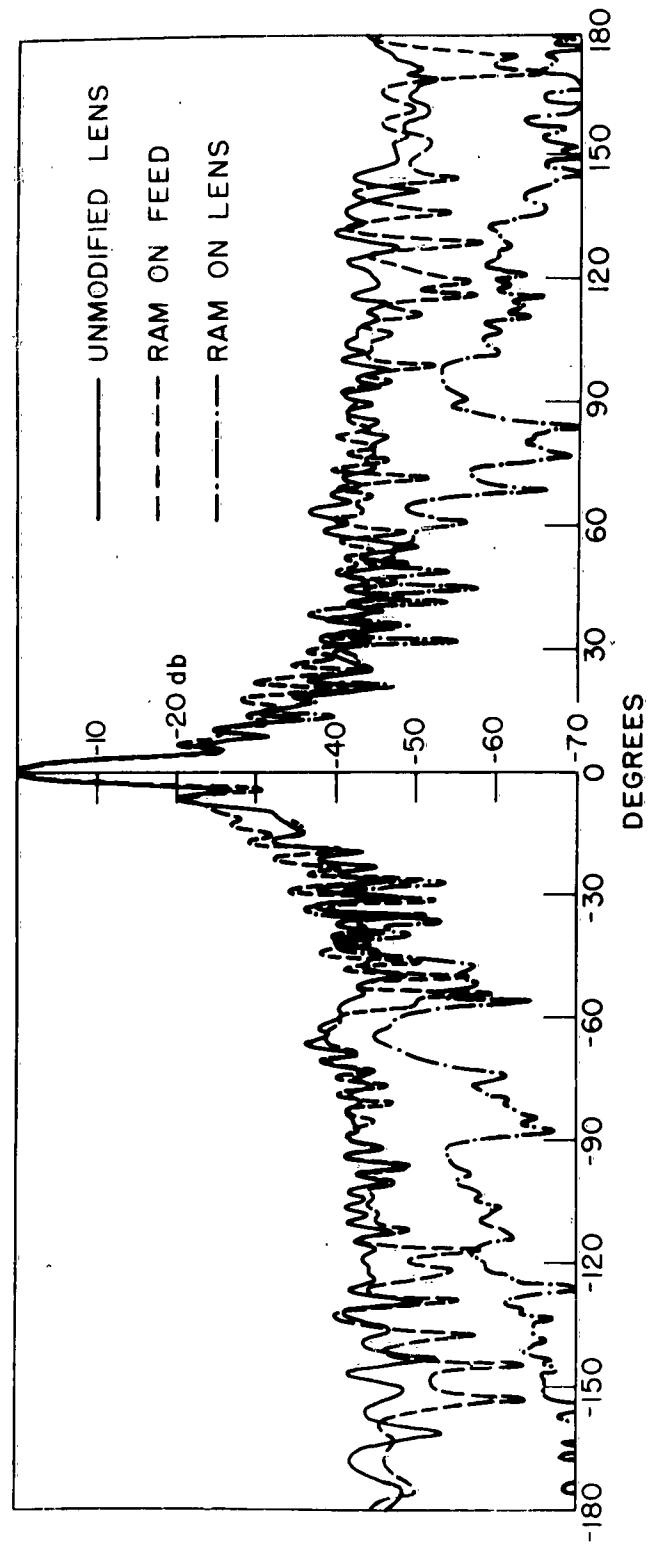


Fig. 16. Luneberg lens antenna patterns.

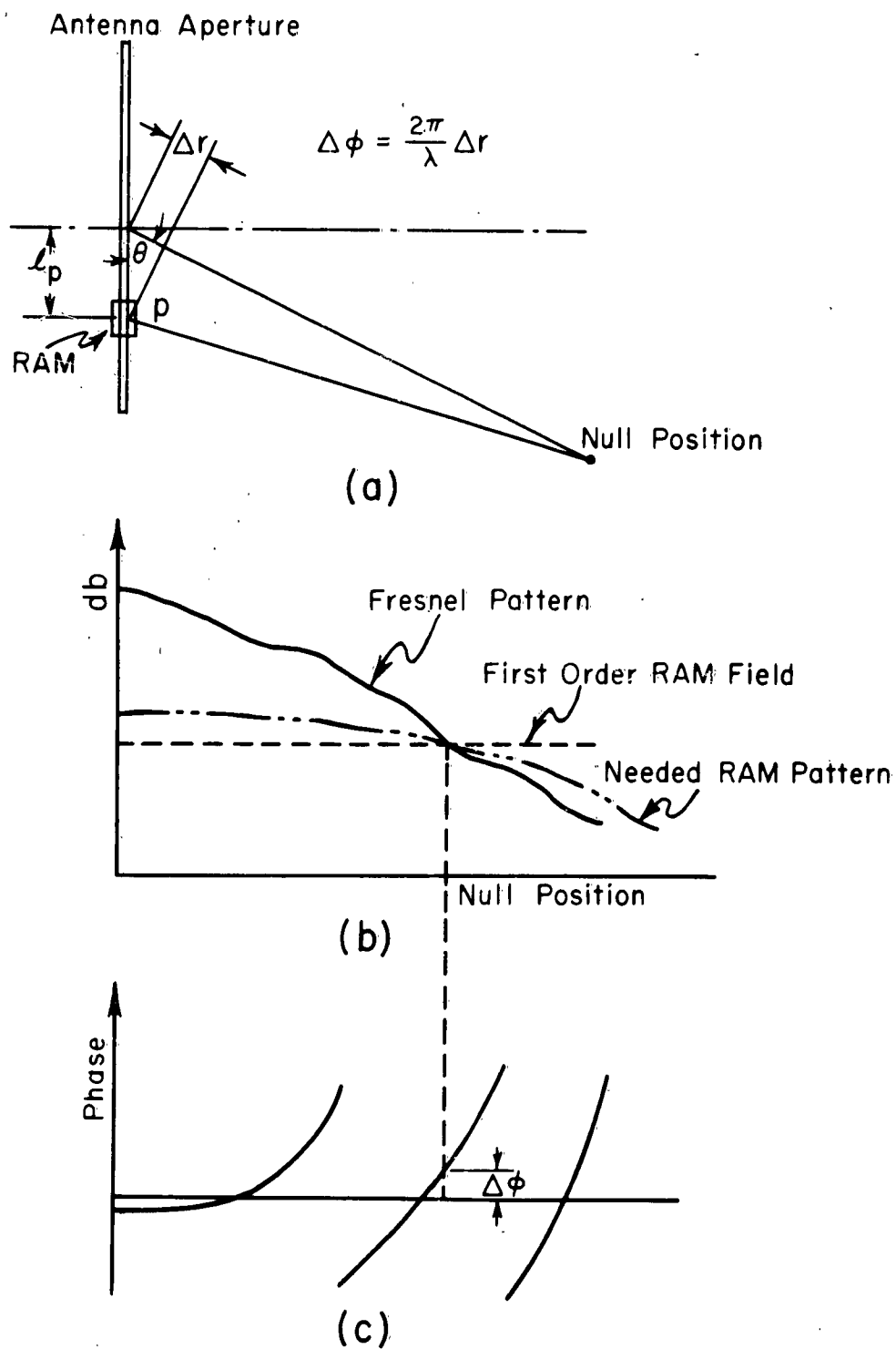


Fig. 17. Method for approximating absorber size and position.

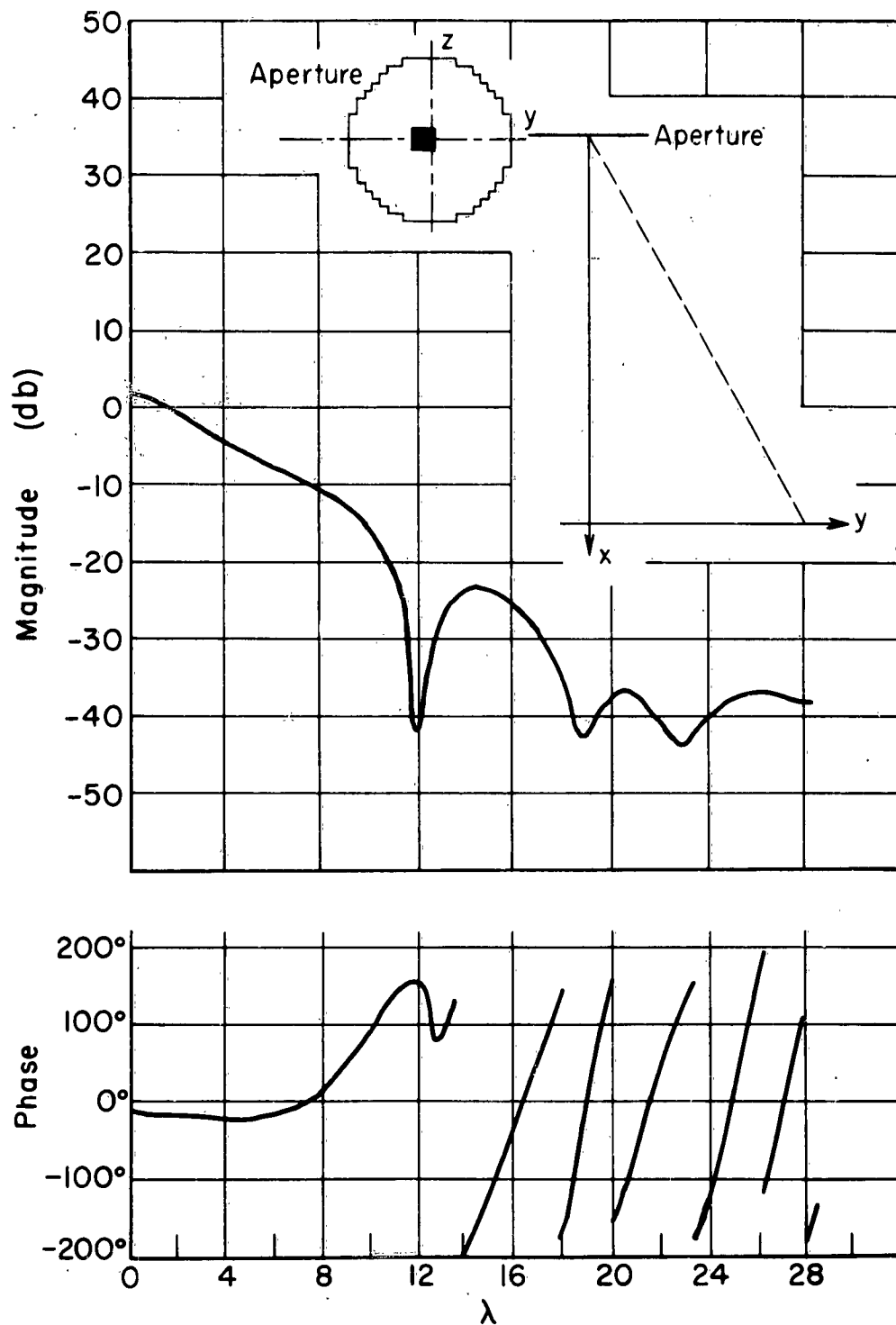


Fig. 18. Fresnel zone pattern with absorber applied (first attempt).

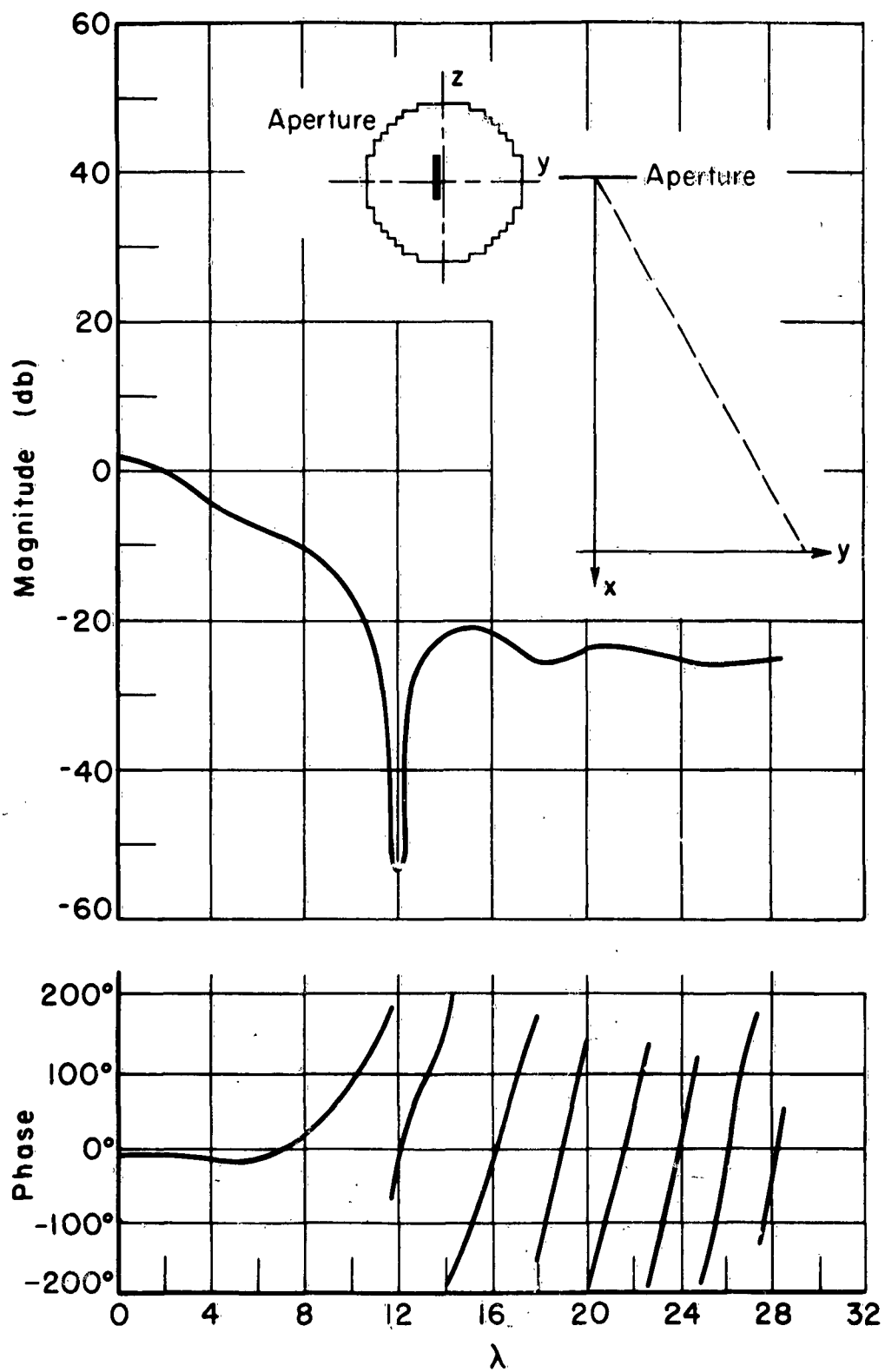


Fig. 19. Fresnel pattern with absorber applied (second attempt).

CATALOGUE FILE CARD

<p>Rome Air Development Center, Griffiss AF Base, N.Y. RADC-TDR-63-133. RFI REDUCTION BY CONTROL OF ANTENNA SIDELOBES. 1 Jan 63, 35pp, incl illus.</p> <p>Unclassified Report</p> <p>This report describes measurements and theoretical developments on the far sidelobes or backlobe region of three basic antenna types: the horn antenna, the parabolic reflector antenna, and the Luneberg lens antenna. The application is for RFI reduction with emphasis on the use of radar absorber materials.</p>	<p>1. Antenna radiation patterns 2. Radio interference I. AFSC Project 4540, Task 454001 II. Contract AF30(602)-2711 III. Ohio State Univ., Antenna Laboratory Columbus 10, Ohio IV. L. Peters, Jr., R.C. Rudduck V. Not in OTS collection VI. In ASTIA collection</p>	<p>Rome Air Development Center, Griffiss AF Base, N.Y. RADC-TDR-63-133. RFI REDUCTION BY CONTROL OF ANTENNA SIDELOBES. 1 Jan 63, 35pp, incl illus.</p> <p>Unclassified Report</p> <p>This report describes measurements and theoretical developments on the far sidelobes or backlobe region of three basic antenna types: the horn antenna, the parabolic reflector antenna, and the Luneberg lens antenna. The application is for RFI reduction with emphasis on the use of radar absorber materials.</p>	<p>1. Antenna radiation patterns 2. Radio interference I. AFSC Project 4540, Task 454001 II. Contract AF30(602)-2711 III. Ohio State Univ., Antenna Laboratory Columbus 10, Ohio IV. L. Peters, Jr., R.C. Rudduck V. Not in OTS collection VI. In ASTIA collection</p>
<p>Rome Air Development Center, Griffiss AF Base, N.Y. RADC-TDR-63-133. RFI REDUCTION BY CONTROL OF ANTENNA SIDELOBES. 1 Jan 63, 35pp, incl illus.</p> <p>Unclassified Report</p> <p>This report describes measurements and theoretical developments on the far sidelobes or backlobe region of three basic antenna types: the horn antenna, the parabolic reflector antenna, and the Luneberg lens antenna. The application is for RFI reduction with emphasis on the use of radar absorber materials.</p>	<p>1. Antenna radiation patterns 2. Radio interference I. AFSC Project 4540, Task 454001 II. Contract AF30(602)-2711 III. Ohio State Univ., Antenna Laboratory Columbus 10, Ohio IV. L. Peters, Jr., R.C. Rudduck V. Not in OTS collection VI. In ASTIA collection</p>	<p>Rome Air Development Center, Griffiss AF Base, N.Y. RADC-TDR-63-133. RFI REDUCTION BY CONTROL OF ANTENNA SIDELOBES. 1 Jan 63, 35pp, incl illus.</p> <p>Unclassified Report</p> <p>This report describes measurements and theoretical developments on the far sidelobes or backlobe region of three basic antenna types: the horn antenna, the parabolic reflector antenna, and the Luneberg lens antenna. The application is for RFI reduction with emphasis on the use of radar absorber materials.</p>	<p>1. Antenna radiation patterns 2. Radio interference I. AFSC Project 4540, Task 454001 II. Contract AF30(602)-2711 III. Ohio State Univ., Antenna Laboratory Columbus 10, Ohio IV. L. Peters, Jr., R.C. Rudduck V. Not in OTS collection VI. In ASTIA collection</p>